

# Towards high-throughput *in situ* structural biology using electron cryotomography

Jan Böhning <sup>a, b</sup>, Tanmay A.M. Bharat <sup>a, b, \*</sup>

<sup>a</sup> Sir William Dunn School of Pathology, University of Oxford, South Parks Road, Oxford OX1 3RE, United Kingdom

<sup>b</sup> Central Oxford Structural Microscopy and Imaging Centre, South Parks Road, Oxford OX1 3RE, United Kingdom

## ARTICLE INFO

### Article history:

Received 17 January 2020

Received in revised form

21 May 2020

Accepted 27 May 2020

Available online 21 June 2020

### Keywords:

cryo-ET

cryo-electron tomography

Electron cryotomography

Sub-tomogram averaging

*in situ* structural biology

## ABSTRACT

Electron cryotomography is a rapidly evolving method for imaging macromolecules directly within the native environment of cells and tissues. Combined with sub-tomogram averaging, it allows structural and cell biologists to obtain sub-nanometre resolution structures *in situ*. However, low throughput in cryo-ET sample preparation and data acquisition, as well as difficulties in target localisation and sub-tomogram averaging image processing, limit its widespread usability. In this review, we discuss new advances in the field that address these throughput and technical problems. We focus on recent efforts made to resolve issues in sample thinning, improvement in data collection speed at the microscope, strategies for localisation of macromolecules using correlated light and electron microscopy and advancements made to improve resolution in sub-tomogram averaging. These advances will considerably decrease the amount of time and effort required for cryo-ET and sub-tomogram averaging, ushering in a new era of structural biology where *in situ* macromolecular structure determination will be routine.

© 2020 The Authors. Published by Elsevier Ltd. This is an open access article under the CC BY license (<http://creativecommons.org/licenses/by/4.0/>).

## 1. Introduction and background

Modern electron microscopes are uniquely suited for the visualisation of biological macromolecules and macromolecular assemblies (Cheng, 2015; Kühlbrandt, 2014). Major difficulties that previously prevented structure determination of macromolecules using electron microscopy have been resolved in recent decades with the advent of electron cryomicroscopy (cryo-EM) (Dubochet et al., 1988), together with advancements in detector technology (Li et al., 2013; McMullan et al., 2016) and the development of sophisticated image processing algorithms (Frank et al., 1996; Grigorieff, 2007; Scheres, 2012). Near-atomic resolution structures of biological macromolecules and complexes can now be routinely solved using cryo-EM (Nogales and Scheres, 2015). The most commonly used cryo-EM structure determination method for biological macromolecules is single particle analysis (SPA), in which numerous two-dimensional (2D) images of isolated macromolecules are acquired in an electron microscope operating at liquid nitrogen temperatures. Each 2D projection of the macromolecule corresponds to a section of its three-dimensional (3D) structure in

Fourier space (Crowther et al., 1970; De Rosier and Klug, 1968). Projections of the macromolecule can be assigned orientations relative to the 3D structure in an iterative process, and used to populate 3D Fourier space, leading to structure solution. SPA is rapidly gaining popularity with structural biologists, since only small amounts of specimen are needed for structure determination and the extensive trials required for 2D or 3D crystallisation can be avoided (Frank, 2006b).

Despite these advantages, SPA still requires at least partial purification of target molecules away from their native environment inside cells and tissues. Biochemical purification is often laborious, and arguably the bottleneck in most structural biology studies. Additionally, high-quality purification is usually needed for structural biology, as impurities may be inadvertently selected alongside target macromolecules in cryo-EM images, confounding the subsequent image processing and leading to spurious structure solution. Perhaps most critically, many target macromolecules are influenced and modified by their cellular environment, and their native 3D structure is often distorted by biochemical purification, meaning that the native conformation only exists in the native environment inside the cell (Baumeister, 2002). In such cases, a specialised application of cryo-EM called electron cryotomography (cryo-ET) may be used to create 3D reconstructions of target molecules directly in their native environment (Baumeister, 2002).

\* Corresponding author. Sir William Dunn School of Pathology, University of Oxford, South Parks Road, Oxford OX1 3RE, United Kingdom.

E-mail address: [tanmay.bharat@path.ox.ac.uk](mailto:tanmay.bharat@path.ox.ac.uk) (T.A.M. Bharat).

Studying biological macromolecules in their cellular context using cryo-ET allows direct visualisation of interactions between complexes and the cellular environment, which are integral to macromolecular function. Recent examples of such studies include the visualisation of proteasome tethering to nuclear pore complexes (Albert et al., 2017), proteasome recruitment in response to poly-GA aggregation (Guo et al., 2018), and the interaction of transcription and translation complexes in bacterial cells (O'Reilly et al., 2020).

In cryo-ET, the sample of interest is imaged using cryo-EM at numerous tilt angles of the goniometer of the specimen stage (Baumeister, 2002; Frank, 2006a). The resulting images have a defined angular relationship with each other according to the tilt angle physically applied to the stage during data collection. This angular information may be used to obtain a computational 3D reconstruction of the specimen known as a tomogram (Koster et al., 1997), containing high-resolution snapshots of molecules, organelles and cells. In this way, samples beyond the reach of the SPA methodology can be studied in their native environment. Cryo-ET has been used in the past to study a variety of complex specimens, including asymmetric viral capsids (Schur et al., 2016), heterogeneous macromolecular assemblies (Brandt et al., 2010), cellular components (Engel et al., 2015a, 2015b; Patla et al., 2010) and whole cells (Chang et al., 2016; Dai et al., 2013; Szwedziak et al., 2014).

Typically, cryo-ET data suffers from low signal-to-noise ratios due to dose limitations related to biological specimens. Another factor contributing to low signal-to-noise ratios is the increased effective thickness of the specimen at high tilt angles. Despite lowered signal-to-noise ratios, high-resolution information is nevertheless preserved within the tilt series images and tomograms. To retrieve this information, copies of the same target macromolecule can be aligned and averaged in a procedure called sub-tomogram averaging (STA) (Beck et al., 2004; Briggs, 2013; Grünwald et al., 2003). In STA, repeated copies of the macromolecule of interest found inside tomograms (called sub-tomograms) are rotationally and translationally aligned in an iterative manner in 3D, and averaged together to produce a higher resolution reconstruction of the target structure, where the correct hand of the target is unambiguously determined (Briggs, 2013). Using STA, the architectures and structures of numerous protein assemblies have been successfully solved directly within their cellular context. For example, the architecture of a bacterial Type IV pilus and its associated molecular machinery (Chang et al., 2016), bacterial surface layer structures (Bharat et al., 2017; von Kügelgen et al., 2020), virus particles budding from mammalian cells (Bharat et al., 2011; Carlson et al., 2008), conformations of proteasome complexes in cells (Asano et al., 2015) and the structure of translating ribosomes in mitochondria (Pfeffer et al., 2015) could be studied using the method. Other success stories include near-atomic resolution structures of viral capsids and membrane proteins that could be solved in recent years from *in vitro* purified samples (Himes and Zhang, 2018; Hutchings et al., 2018), underlining the feasibility of the method for determining high-resolution structures *in situ*.

Despite the promise of STA to resolve *in situ* structures, the technique suffers from a number of disadvantages compared to SPA. The major limiting factor is the substantial time and effort typically required for all aspects of the cryo-ET and STA workflow, including sample preparation, image acquisition and image processing. In particular, one aspect of this bottleneck is the preparation of suitable specimens of cellular samples that are inherently thick, often spanning several micrometres. This bottleneck is typically circumvented by thinning of the specimen using laborious genetics or advanced sample preparation approaches, which are costly and time-intensive. Another bottleneck in the cryo-ET workflow is the localisation of targets within the bewildering

complexity of a cell, often limiting *in situ* structural studies to a handful of the largest of cellular complexes, such as ribosomes, microtubules and proteasomes (Grange et al., 2017; Guo et al., 2018; Mahamid et al., 2016). Next, the acquisition of tomographic data on the electron microscope, typically requiring 40–120 tilt images per tomogram, is an order of magnitude slower when compared to SPA (Hagen et al., 2017). Given that tomography requires more expensive 300 kV microscopes to image relatively thick target samples, this is a particular challenge in the current environment, where time on such machines is at a premium (Bharat and Kukulski, 2019). Finally, STA is relatively time-consuming compared to SPA, with several image processing steps, which perhaps precludes its widespread application in the structural biology field.

In this review article, we examine the key bottlenecks and challenges in every step of the cryo-ET workflow, including sample preparation, data acquisition and image processing, that prevent routine high-resolution structure determination inside cells and tissues. We outline current efforts within the community to resolve these throughput and technical issues, and discuss the future that lies ahead for *in situ* structural biology.

### 1.1. Sample preparation for cryo-ET

To acquire high-quality cryo-ET data, the first step is the preparation of a suitably thin specimen that allows the electron beam to penetrate through it and provide images with adequate quality. Practically, cryo-EM images of samples thicker than ~400 nm suffer from significantly reduced signal-to-noise ratios due to increased inelastic scattering events of the incident electrons (McIntosh et al., 2005). Therefore, specimen thickness is an important factor to be considered for sample preparation in cellular cryo-ET. Because of this consideration, much of the early cryo-ET work was conducted on viruses and thin bacterial cells that met this criterion (Cyrklaff et al., 2005; Grünwald et al., 2003; Kürner et al., 2005). For thicker bacteria, researchers have devised genetic engineering tools to further reduce cell size and thickness or produce 'mini-cells' before vitrification through plunge freezing in liquid ethane (Melia and Bharat, 2018; Park et al., 2018). Genetic systems and mutants that result in reduced cell sizes are, however, not established for every species, limiting the applicability of this approach. For eukaryotic cells, which are commonly several micrometres thick, only the edges of cells are directly amenable to cryo-ET (Bharat et al., 2011; Grange et al., 2017). Sometimes biochemical isolation of organelles of interest or other sub-cellular features is possible, and aids in the preparation of a thin specimen suitable for cryo-EM (Beck et al., 2004; Nicastro et al., 2000). However, specimens isolated in this way are significantly perturbed from their native state, which could lead to spurious artefacts that confound biological interpretation.

To visualise target macromolecules in thick cells with limited perturbation of the system, sample thinning is usually employed after vitrification of the specimen (post-vitrification). A classical approach for post-vitrification sample thinning is mechanical sectioning using a diamond knife, also known as cryo-EM of vitreous sections (CEMOVIS) (Al-Amoudi et al., 2004). CEMOVIS has been successfully applied to a variety of samples including bacteria (Salje et al., 2009), yeast (Bharat et al., 2018) and human cells (Al-Amoudi et al., 2007). CEMOVIS is widely applicable and each section contains multiple targets for data collection due to the large surface area of the section (Bharat and Kukulski, 2019). CEMOVIS, however, suffers from several important drawbacks, in particular, the process of sectioning is extremely labour intensive, and specialised expertise is needed for producing high-quality sections. Perhaps more importantly, diamond knife sectioning introduces artefacts to the specimen, which diminish the achievable resolution

in cryo-ET (Pierson et al., 2011). This last drawback arguably precludes CEMOVIS for routine *in situ* structural biology applications where high-resolution macromolecular structures are needed to answer the biological question at hand.

A method for preparing thin cellular samples post-vitrification which is rapidly gaining in popularity is focused ion beam (FIB) milling (Marko et al., 2007). In FIB milling, a stream of charged metal ions (usually gallium ions) is used to ablate the vitrified specimen above and below the area of interest, leaving a thin 'lamella' with a significantly reduced thickness of ~100–200 nm that is amenable to high-resolution cryo-ET studies. This technique has been shown to be a powerful tool to reveal the organisation of protein complexes and organelles within cells (Guo et al., 2018; Hoffmann et al., 2019; Lopez-Garrido et al., 2018) even within the thickest parts of eukaryotic cells, such as the nucleus (Mahamid et al., 2016). While enormously useful for cellular studies, a major limitation of FIB milling is its low throughput. There are several cryo-handling steps involved in the workflow before the sample reaches the transmission electron microscope (TEM) for cryo-ET data collection, including initial vitrification, transfers in and out of a FIB-SEM (scanning electron microscope) and transfer to a TEM. Furthermore, the FIB milling step itself typically requires a lot of manual attention and regular user input. To obtain a sufficient number of tomograms, several high-quality lamellae are often required, needing hundreds of work hours at the FIB-SEM. This makes the workflow cumbersome and suitable only to a handful of biological problems. To overcome this bottleneck, an automated lamella preparation protocol has been recently developed, which greatly reduces user input and work hours required (Marko et al., 2007; Zachs et al., 2019). Using this new automated setup for sample preparation, the structure of bacterial gap junctions in cyanobacteria was solved using an unprecedentedly large dataset acquired from ~120 lamellas (Fig. 1A) (Weiss et al., 2019). Since low abundance is a key limitation for many cellular targets, and lamellae only capture a thin section of a cell, automation will greatly aid the feasibility of *in situ* structural biology using FIB milling and can be expected to gain popularity in the future.

## 1.2. Data acquisition on the TEM

Since cryo-ET data are collected as a series of tilted images, data acquisition is considerably slower compared to SPA. Given the limited availability of measurement time on high-end microscopes, this is a major limiting factor for many studies. Furthermore, if the target macromolecule is present in several functional states in the specimen, data required to reach the desired resolution in downstream STA multiplies accordingly, making many projects unfeasible. To overcome this, a concerted effort needs to be made to reduce cryo-ET data collection time at the microscope.

In the case of vitreous sections thinned by CEMOVIS, sections have a tendency to move during cryo-ET data acquisition (Pierson et al., 2011). Specimen movement of sections is a huge problem since the feature of interest moves out of the field of view during the tilt series, rendering the data unusable. This severely limits the throughput of cryo-ET data collection and subsequent STA. This problem of section movement has been recently resolved by adding a cryo-light microscopy (cryo-LM) pre-screening step to identify deposited sections that are well-adhered to the grid (Bharat et al., 2018), significantly improving data throughput. Using this approach, vitreous sections well-adhered to the grids were consistently identified, leading to near perfect success rate of all tilt series collected (Bharat et al., 2018), and a considerable increase in data usable for STA.

When STA reaches higher, typically sub-nanometre resolutions, specimen movement induced by the electron beam also becomes

problematic, as shown by pioneering SPA cryo-EM studies (Brilot et al., 2012). For cryo-ET, this problem has also been highlighted by comparing SPA and STA performed on the same specimen of Hepatitis B virus capsids, where specimen movement lead to blurring of higher resolution features in tomograms, leading to substantially worse STA refinement (Bharat et al., 2015). Another experiment where the same SPA and STA methods were applied to characteristically shaped DNA origami particles confirmed that both translational as well as rotational movement of the specimen occurred during tilt series data acquisition (Bharat et al., 2015). While specimen movement within single tilt images can be corrected by the acquisition of movies (Fromm et al., 2015; Scheres, 2014), repeated movements of the specimen throughout tilt series collection cannot be easily corrected and significantly limits resolution in cryo-ET and STA. An obvious solution to this issue is to find methods to prevent radiation-induced specimen motion at the microscope in the first place. One innovative way to resolve the problem is through the use of ultrastable gold substrates for sample preparation (Russo and Passmore, 2014), which leads to improved outcomes in STA due to reduced specimen movement during tilt series data acquisition (Bharat et al., 2015).

Pre-screening for suitable specimen sections using a cryo-light microscope or using ultrastable gold substrates are strategies that can be adopted before actual cryo-ET data acquisition to improve the success rate at the microscope. Once the sample has reached the microscope, the use of dose-symmetric tilt schemes further improves data quality (Hagen et al., 2017), leading to much improved STA maps with the same amount of data (Turoňová et al., 2020). Dose-symmetric tilt schemes have now been implemented in popular data collection software packages including SerialEM (Mastronarde, 2005), increasing the accessibility of the strategy to laboratories seeking to improve the quality of their cryo-ET data.

Another inventive method to significantly improve data collection rates at the microscope is the continuous tilt scheme, where images are captured while continuously tilting the stage progressively through the tilt range (Chreifi et al., 2019). This method allows the acquisition of tilt series in a much shorter time compared to conventional tilting schemes (Chreifi et al., 2019). While continuous goniometer rotation for tilted data collection is well-known in the X-ray crystallography field (Brönnimann et al., 2003), the requirements for cryo-ET are more stringent. Whereas crystals may be several micrometres in size and slight translation of the goniometer does not alter the diffraction pattern, cryo-ET is more demanding as features of interest must remain centred within the field of view during tilt series acquisition, a considerable challenge at high magnifications. The acquisition of tilt series data using the continuous tilt scheme was enabled by the use of sample holders with improved eucentricity. Although features remained within the field of view during data acquisition, the original, ideal continuous tilt scheme was found to be incompatible with high-resolution cryo-ET (>3 nm resolution) due to motor vibrations induced during continuous tilting (Fig. 1B) (Chreifi et al., 2019). This fact prompted the development of fast-incremental tilt schemes, which briefly stop goniometer movement during continuous tilt acquisition but omit tracking, autofocus, tilt-backlash correction and settling times, yielding sub-nanometre structures with less than an hour of total acquisition time (Eisenstein et al., 2019). With the development of faster and larger detectors such as the K3 (Gatan Inc.) and more stable sample stages, data collection in fully continuous mode for high-resolution structure determination might become routine, considerably increasing throughput, and promising a bright future for the cryo-ET field. Such developments could also be fruitful for SPA, given that tomograms acquired after the single-particle micrograph could yield valuable information about the specimen, such as symmetry (Bharat et al., 2012) or



## Improvements in cryo-ET for *in situ* structural biology

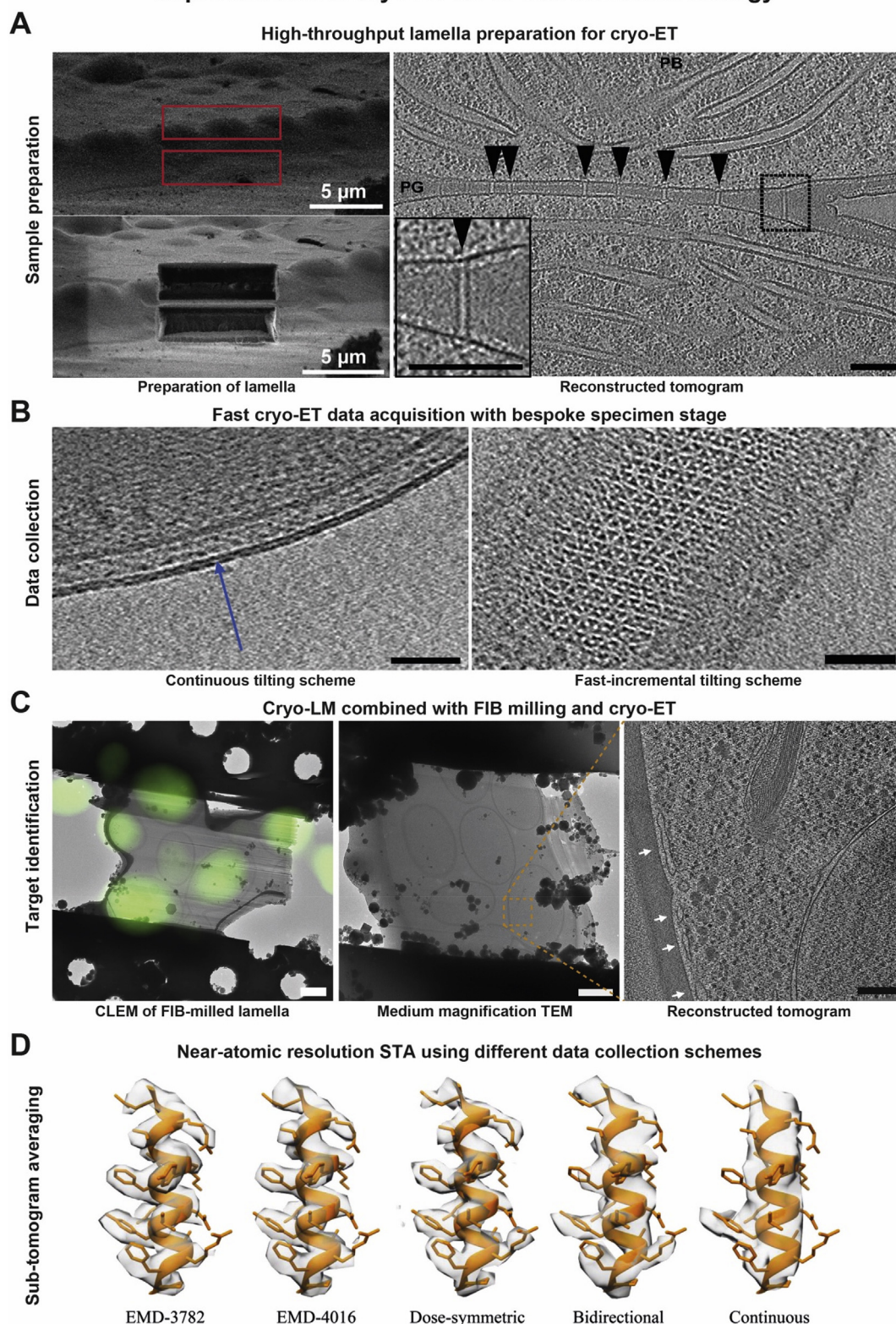


**Fig. 1.** Recent breakthroughs in cryo-ET in sample preparation, data acquisition, target identification and STA.

A) High-throughput lamella production. Left: Before (upper) and after (lower) lamella preparation via FIB milling of a cyanobacterial filament. Right: XY slice through a cryo-tomogram depicting the septum of two *Anabaena* cyanobacteria cells. Arrows mark septal junctions. One septal junction is shown magnified (inset). Scale bars: 100 nm. PG – septal peptidoglycan, PB – phycobilisome. Adapted from (Weiss et al., 2019).

B) Visualisation of cellular features using two fast tilt scheme variants. Left: Two leaflets of the outer membrane lipid bilayer of *Bdellovibrio bacteriovorus* (blue arrow) resolved using a continuous tilt scheme, yielding ~4 nm resolution. Right: Tomographic slice generated from fast-incremental tilt scheme data reveals a methyl-accepting chemotaxis protein array in *Bdellovibrio bacteriovorus*, at a quality similar to conventional tilt schemes but acquired considerably faster. Scale bars: 50 nm. Adapted from (Chreifi et al., 2019).

C) CLEM of budding yeast cells expressing a fluorescent marker for elevated calcium levels. Elevated intracellular calcium, as quantified via strength of the fluorescence signal,

adherence to the air-water interface (Bharat and Scheres, 2016; Noble et al., 2018).

### 1.3. Identification of targets in cells

A considerable problem for *in situ* structural biology is the identification of targets within the crowded environment of the cell. Unlike cryo-EM SPA, which makes use of purified and therefore biochemically defined samples, the cellular environment is a heterogeneous and complex space, where thousands of different macromolecules can be present in a variety of conformations. For all but the most abundant of complexes, the identification of target macromolecules is a difficult and time-consuming, yet vital task required for the success of any cryo-ET and STA study. The localisation of macromolecular complexes in the cellular environment at high resolution provides additional valuable information about macromolecular function, enriching the structural biology information gleaned from STA. It can thus provide a contextual understanding to facilitate accurate modelling of the cellular environment at high resolution, which is of immense importance to cell biology and an important goal for the cryo-ET community.

Previous cryo-ET studies often used abundant and easily identifiable targets for STA. Examples of these include retrovirus capsid proteins (Turoňová et al., 2020), bacterial S-layers (Bharat et al., 2017; Gambelli et al., 2019; von Kügelgen et al., 2020) or ribosomes (Pfeffer et al., 2015). These targets either form supramolecular repeating arrays on membranes or are comparatively large and easy to discern in a straight-forward manner by a simple visual inspection of tomograms. For smaller complexes that are not arranged in a predictable way such as a supramolecular lattice, identification within tomograms is challenging and requires an additional localisation step to determine their exact position within the cell.

A popular method to facilitate localisation of macromolecules in EM images is to add a fluorescent label to the target and locate it in a cryo-LM step prior to obtaining cryo-EM data. Several laboratories have shown that high-accuracy correlated light and electron microscopy (CLEM) is feasible (Chang et al., 2014; Schellenberger et al., 2014; Schorb et al., 2017), allowing identification of targets using cryo-LM images as guide for electron microscopy. Cryo-CLEM approaches are fully compatible with thicker samples, and have been performed together with CEMOVIS (Bharat et al., 2018), and also with FIB milling (Fig. 1C) (Arnold et al., 2016; Guo et al., 2018; Hoffmann et al., 2019; Watanabe et al., 2019). A new methodology that integrates a light microscopy objective inside a FIB-SEM, allowing simultaneous milling and target localisation, was reported recently (Gorelick et al., 2019). Such integrated machines may be important in the future for efficient target identification by providing important feedback during the thinning process, increasing the overall success rate of cryo-ET studies.

Fluorescent tagging is not always possible for every macromolecular complex, because it can disrupt macromolecular localisation and function. Even if cryo-LM has been performed, the exact localisation and orientation of the target complex within the tomogram may not be obvious, particularly for smaller targets. In such situations, the cryo-EM signal from the target complex itself, as present in the tomogram, must be used for identification. In some cases complexes can be identified by template-free pattern mining (Martinez-Sanchez et al., 2020; Xu et al., 2019), but are more typically obtained by providing a template that is used to

mine tomographic volumes (Frangakis et al., 2002), often involving state-of-the-art algorithms, such as supervised neural networks (Chen et al., 2017). To describe the most typical case, called template matching, low-resolution features of a previously known atomic structure of the target macromolecule are compared with the tomogram, leading to predictions for locations of the target in the tomographic volume by cross-correlation or another figure of merit (Frangakis et al., 2002). Misidentification or incorrect assignment of cross-correlation peaks remains problematic, however, particularly for smaller targets where contrast is poor. Despite these issues, template or pattern matching will likely play an important role in the future with ever-increasing data quality and throughput, especially since target identification requires no additional experimentation. Therefore, to ultimately solve the problem of protein detection in cryo-ET, both novel approaches in structural pattern mining (Wu et al., 2019) and higher quality data delivered by modern detectors and microscopes will be required to enable studies of smaller targets. This remains a challenge for the cryo-ET field, and is the focus of efforts in many laboratories.

### 1.4. STA image processing

To resolve structural detail from macromolecular complexes identified in cryo-ET data using the methods detailed above, STA image processing must be performed. STA is analogous to SPA, where multiple copies of the target macromolecule are averaged (Briggs, 2013). STA is completely synergistic with SPA, and several studies have shown how these methodologies can inform the other to guide higher resolution reconstructions (Bharat et al., 2012, 2013; Song et al., 2020). Compared to SPA however, STA is not widely used, and typically only applied in specialised cases. This is partly due to the increased complexity of image processing in STA, consisting of several steps, from tomographic reconstruction to sub-tomogram alignment and averaging. While a number of tools exist that enhance the power of STA, a patchwork of different software and computational tools is usually required to go from movies collected on the microscope to a high-resolution structure. This makes STA considerably more time-consuming than SPA, where several user-friendly pipelines exist that guide users through all aspects of processing (Grant et al., 2018; Scheres, 2012). To overcome the issue of usability, several laboratories are now developing image processing pipelines that include initial data processing, tomogram reconstruction and STA in the same computational package. Examples of such programs include (but are not limited to) IMOD (Kremer et al., 1996), EMAN2 (Tang et al., 2007), emClarity (Himes and Zhang, 2018), PyTom (Hrabe et al., 2012) and Warp (Tegunov and Cramer, 2019). It is hoped that such streamlining will encourage use of STA as a technique for structural solution.

A major issue with STA is that obtained final resolutions of macromolecular structures are often significantly lower than in SPA studies, perhaps limiting the popularity of STA. For *in vitro* purified specimens, it has been shown that STA is able to produce sub-4 Å resolution structures (see Fig. 1D) (Turoňová et al., 2020), but there are several resolution-limiting aspects unique to cryo-ET and STA to consider. For near-atomic resolution STA, the accuracy of CTF estimation and compensation considerably influences the attainable resolution. In stark contrast to SPA, however, a single defocus value cannot be assumed for CTF compensation of single tilt images, complicating CTF estimation and compensation. Several packages now include per-sub-tomogram CTF compensation (Bharat et al.,

guided tomogram acquisition, and subsequent analysis of extended synaptotagmins bridging the endoplasmic reticulum and the plasma membrane. Scale bars: 2 µm (left and middle), 200 nm (right). Adapted from (Hoffmann et al., 2019).

D) High-resolution sub-tomogram averaging of HIV capsid-SP1 using different tilt schemes. Atomic structure shown as a ribbon diagram built into the resolved density. The dose-symmetric tilt scheme results in the highest resolution reconstruction, where side chains are clearly resolved. Adapted from (Turoňová et al., 2020).



2015; Chen et al., 2019), which allows high-resolution structures to be obtained. Recently, novel defocus-gradient CTF compensation algorithms have been reported, as implemented by NovaCTF and emClarity (Himes and Zhang, 2018; Turoňová et al., 2017). Using these, structures of retroviral Gag proteins could be resolved at resolutions higher than 3.5 Å. These novel algorithms, along with others, will increase the power of STA and pave the way for widespread applicability of cryo-ET and STA, and lead to routine *in situ* structure determination to reveal novel insights into otherwise inaccessible biological problems.

## 2. Conclusion

Solving macromolecular structures in cells using cryo-ET and STA has been shown to be feasible in recent years. The widespread use of cryo-ET and STA however, has been prevented by the time-consuming and laborious nature of the workflow, including low throughput in sample preparation, slow data acquisition speeds, difficulties in target identification, and limited usability of image processing software. Several proof-of-concept studies have addressed these problems in recent years, improving significantly upon each aspect of the workflow. These novel strategies promise to elevate *in situ* structural biology in the long-term to a valuable tool for both the structural and cell biologist.

## Declaration of competing interest

The authors declare no conflict of interest.

## Acknowledgments

We apologise to all our colleagues whose work could not be cited due to space restraints. T.A.M.B. is a recipient of a Sir Henry Dale Fellowship, jointly funded by the Wellcome Trust and the Royal Society (202231/Z/16/Z). T.A.M.B. would like to thank the Vallee Research Foundation, Action Medical Research Charity for Children (grant GN2634), the Cystic Fibrosis trust and the John Fell Fund for support. J.B. is supported by a Medical Research Council graduate studentship. The authors would like to thank Dr. Charlotte Melia for critically reading the manuscript.

## References

- Al-Amoudi, A., Chang, J.J., Leforestier, A., McDowall, A., Salamin, L.M., Norlen, L.P., Richter, K., Blanc, N.S., Studer, D., Dubochet, J., 2004. Cryo-electron microscopy of vitreous sections. *EMBO J.* 23, 3583–3588.
- Al-Amoudi, A., Diez, D.C., Betts, M.J., Frangakis, A.S., 2007. The molecular architecture of cadherins in native epidermal desmosomes. *Nature* 450, 832–837.
- Albert, S., Schaffer, M., Beck, F., Mosalaganti, S., Asano, S., Thomas, H.F., Plitzko, J.M., Beck, M., Baumeister, W., Engel, B.D., 2017. Proteasomes tether to two distinct sites at the nuclear pore complex. *Proc. Natl. Acad. Sci. U. S. A.* 114, 13726–13731.
- Arnold, J., Mahamid, J., Lucic, V., de Marco, A., Fernandez, J.J., Laugks, T., Mayer, T., Hyman, A.A., Baumeister, W., Plitzko, J.M., 2016. Site-specific cryo-focused ion beam sample preparation guided by 3D correlative microscopy. *Biophys. J.* 110, 860–869.
- Asano, S., Fukuda, Y., Beck, F., Aufderheide, A., Förster, F., Danev, R., Baumeister, W., 2015. Proteasomes. A molecular census of 26S proteasomes in intact neurons. *Science* 347, 439–442.
- Baumeister, W., 2002. Electron tomography: towards visualizing the molecular organization of the cytoplasm. *Curr. Opin. Struct. Biol.* 12, 679–684.
- Beck, M., Förster, F., Ecke, M., Plitzko, J.M., Melchior, F., Gerisch, G., Baumeister, W., Medalia, O., 2004. Nuclear pore complex structure and dynamics revealed by cryoelectron tomography. *Science* 306, 1387–1390.
- Bharat, T.A., Davey, N.E., Ulbrich, P., Riches, J.D., de Marco, A., Rumlova, M., Sachse, C., Ruml, T., Briggs, J.A., 2012. Structure of the immature retroviral capsid at 8 Å resolution by cryo-electron microscopy. *Nature* 487, 385–389.
- Bharat, T.A., Riches, J.D., Kolesnikova, L., Welsch, S., Krähling, V., Davey, N., Parsy, M.L., Becker, S., Briggs, J.A., 2011. Cryo-electron tomography of Marburg virus particles and their morphogenesis within infected cells. *PLoS Biol.* 9, e1001196.
- Bharat, T.A., Scheres, S.H., 2016. Resolving macromolecular structures from electron cryo-tomography data using subtomogram averaging in RELION. *Nat. Protoc.* 11, 2054–2065.
- Bharat, T.A., Zbaida, D., Eisenstein, M., Frankenstein, Z., Mehlman, T., Weiner, L., Sorzano, C.O.S., Barak, Y., Albeck, S., Briggs, J.A., 2013. Variable internal flexibility characterizes the helical capsid formed by agrobacterium VirE2 protein on single-stranded DNA. *Structure* 21, 1158–1167.
- Bharat, T.A.M., Hoffmann, P.C., Kukulski, W., 2018. Correlative microscopy of vitreous sections provides insights into BAR-domain organization *in situ*. *Structure* 26, 879–886 e873.
- Bharat, T.A.M., Kukulski, W., 2019. Cryo-Correlative Light and Electron Microscopy: toward *in situ* Structural Biology. In: Verkade, P., Collinson, L. (Eds.), *Correlative Imaging: Focusing on the Future*. Wiley.
- Bharat, T.A.M., Kureisaite-Ciziene, D., Hardy, G.G., Yu, E.W., Devant, J.M., Hagen, W.J.H., Brun, Y.V., Briggs, J.A.G., Löwe, J., 2017. Structure of the hexagonal surface layer on *Caulobacter crescentus* cells. *Nat. Microbiol.* 2, 17059.
- Bharat, T.A.M., Russo, C.J., Löwe, J., Passmore, L.A., Scheres, S.H.W., 2015. Advances in single-particle electron cryomicroscopy structure determination applied to sub-tomogram averaging. *Structure* 23, 1743–1753.
- Brandt, F., Carlson, L.A., Hartl, F.U., Baumeister, W., Grünwald, K., 2010. The three-dimensional organization of polyribosomes in intact human cells. *Mol. Cell.* 39, 560–569.
- Briggs, J.A., 2013. Structural biology *in situ*—the potential of subtomogram averaging. *Curr. Opin. Struct. Biol.* 23, 261–267.
- Brilot, A.F., Chen, J.Z., Cheng, A., Pan, J., Harrison, S.C., Potter, C.S., Carragher, B., Henderson, R., Grigorieff, N., 2012. Beam-induced motion of vitrified specimen on holey carbon film. *J. Struct. Biol.* 177, 630–637.
- Brönnimann, C., Eikenberry, E., Horisberger, R., Hülsen, G., Schmitt, B., Schulze-Bries, C., Tomizaki, T., 2003. Continuous sample rotation data collection for protein crystallography with the PILATUS detector. *Nucl. Instrum. Methods Phys. Res. Sect. A Accel. Spectrom. Detect. Assoc. Equip.* 510, 24–28.
- Carlson, L.A., Briggs, J.A., Glass, B., Riches, J.D., Simon, M.N., Johnson, M.C., Müller, B., Grünwald, K., Kräusslich, H.G., 2008. Three-dimensional analysis of budding sites and released virus suggests a revised model for HIV-1 morphogenesis. *Cell Host Microbe* 4, 592–599.
- Chang, Y.W., Chen, S., Tocheva, E.I., Treuner-Lange, A., Lobach, S., Sogaard-Andersen, L., Jensen, G.J., 2014. Correlated cryogenic photoactivated localization microscopy and cryo-electron tomography. *Nat. Methods* 11, 737–739.
- Chang, Y.W., Rettberg, L.A., Treuner-Lange, A., Iwasa, J., Sogaard-Andersen, L., Jensen, G.J., 2016. Architecture of the type IVa pilus machine. *Science* 351, aad2001.
- Chen, M., Bell, J.M., Shi, X., Sun, S.Y., Wang, Z., Ludtke, S.J., 2019. A Complete Data Processing Workflow for CryoET and Subtomogram Averaging arXiv preprint arXiv:190203978.
- Chen, M., Dai, W., Sun, S.Y., Jonasch, D., He, C.Y., Schmid, M.F., Chiu, W., Ludtke, S.J., 2017. Convolutional neural networks for automated annotation of cellular cryo-electron tomograms. *Nat. Methods* 14, 983.
- Cheng, Y., 2015. Single-particle cryo-EM at crystallographic resolution. *Cell* 161, 450–457.
- Chreifi, G., Chen, S., Metskas, L.A., Kaplan, M., Jensen, G.J., 2019. Rapid tilt-series acquisition for electron cryotomography. *J. Struct. Biol.* 205, 163–169.
- Crowther, R.A., DeRosier, D., Klug, A., 1970. The reconstruction of a three-dimensional structure from projections and its application to electron microscopy. *Proceedings of the Royal Society of London A Mathematical and Physical Sciences* 317, 319–340.
- Cyrklaff, M., Risco, C., Fernandez, J.J., Jimenez, M.V., Esteban, M., Baumeister, W., Carrascosa, J.L., 2005. Cryo-electron tomography of vaccinia virus. *Proc. Natl. Acad. Sci. U. S. A.* 102, 2772–2777.
- Dai, W., Fu, C., Raytcheva, D., Flanagan, J., Khant, H.A., Liu, X., Rochat, R.H., Haase-Pettingell, C., Piret, J., Ludtke, S.J., et al., 2013. Visualizing virus assembly intermediates inside marine cyanobacteria. *Nature* 502, 707–710.
- De Rosier, D.J., Klug, A., 1968. Reconstruction of three dimensional structures from electron micrographs. *Nature* 217, 130–134.
- Dubochet, J., Adrian, M., Chang, J.J., Homo, J.C., Lepault, J., McDowall, A.W., Schultz, P., 1988. Cryo-electron microscopy of vitrified specimens. *Q. Rev. Biophys.* 21, 129–228.
- Eisenstein, F., Danev, R., Pilhofer, M., 2019. Improved applicability and robustness of fast cryo-electron tomography data acquisition. *J. Struct. Biol.* 208, 107–114.
- Engel, B.D., Schaffer, M., Albert, S., Asano, S., Plitzko, J.M., Baumeister, W., 2015a. *In situ* structural analysis of Golgi intracisternal protein arrays. *Proc. Natl. Acad. Sci. U. S. A.* 112, 11264–11269.
- Engel, B.D., Schaffer, M., Kuhn Cuellar, L., Villa, E., Plitzko, J.M., Baumeister, W., 2015b. Native architecture of the *Chlamydomonas* chloroplast revealed by *in situ* cryo-electron tomography. *Elife* 4.
- Frangakis, A.S., Böhm, J., Förster, F., Nickell, S., Nicastro, D., Typke, D., Hegerl, R., Baumeister, W., 2002. Identification of macromolecular complexes in cryo-electron tomograms of phantom cells. *Proc. Natl. Acad. Sci. U. S. A.* 99, 14153–14158.
- Frank, J., 2006a. *Electron Tomography*, 2 edn. New York: Springer-Verlag, New York.
- Frank, J., 2006b. *Three-dimensional Electron Microscopy of Macromolecular Assemblies: Visualization of Biological Molecules in Their Native State*. Oxford University Press.
- Frank, J., Radermacher, M., Penczek, P., Zhu, J., Li, Y., Ladjadj, M., Leith, A., 1996. SPIDER and WEB: processing and visualization of images in 3D electron microscopy and related fields. *J. Struct. Biol.* 116, 190–199.
- Fromm, S.A., Bharat, T.A., Jakobi, A.J., Hagen, W.J., Sachse, C., 2015. Seeing tobacco

- mosaic virus through direct electron detectors. *J. Struct. Biol.* 189, 87–97.
- Gambelli, L., Meyer, B.H., McLaren, M., Sanders, K., Quax, T.E.F., Gold, V.A.M., Albers, S.V., Daum, B., 2019. Architecture and modular assembly of *Sulfolobus* S-layers revealed by electron cryotomography. *Proc. Natl. Acad. Sci. U. S. A.* 116, 25278–25286.
- Gorelick, S., Buckley, G., Gervinskis, G., Johnson, T.K., Handley, A., Caggiano, M.P., Whisstock, J.C., Pocock, R., de Marco, A., 2019. PIE-scope, integrated cryo-correlative light and FIB/SEM microscopy. *Elife* 8.
- Grange, M., Vasisht, D., Grünwald, K., 2017. Cellular electron cryo tomography and in situ sub-volume averaging reveal the context of microtubule-based processes. *J. Struct. Biol.* 197, 181–190.
- Grant, T., Rohou, A., Grigorieff, N., 2018. cisTEM, user-friendly software for single-particle image processing. *Elife* 7, e35383.
- Grigorieff, N., 2007. FREALIGN: high-resolution refinement of single particle structures. *J. Struct. Biol.* 157, 117–125.
- Grünwald, K., Desai, P., Winkler, D.C., Heymann, J.B., Belnap, D.M., Baumeister, W., Steven, A.C., 2003. Three-dimensional structure of herpes simplex virus from cryo-electron tomography. *Science* 302, 1396–1398.
- Guo, Q., Lehmer, C., Martinez-Sanchez, A., Rudack, T., Beck, F., Hartmann, H., Perez-Berlanga, M., Frotin, F., Hipp, M.S., Hartl, F.U., et al., 2018. In situ structure of neuronal C9orf72 poly-GA aggregates reveals proteasome recruitment. *Cell* 172, 696–705 e612.
- Hagen, W.J., Wan, W., Briggs, J.A., 2017. Implementation of a cryo-electron tomography tilt-scheme optimized for high resolution subtomogram averaging. *J. Struct. Biol.* 197, 191–198.
- Himes, B.A., Zhang, P., 2018. emClarity: software for high-resolution cryo-electron tomography and subtomogram averaging. *Nat. Methods* 15, 955.
- Hoffmann, P.C., Bharat, T.A.M., Wozny, M.R., Boulanger, J., Miller, E.A., Kukulski, W., 2019. Tricalbins contribute to cellular lipid flux and form curved ER-PM contacts that are bridged by rod-shaped structures. *Dev. Cell* 51, 488–502 e488.
- Hrabe, T., Chen, Y., Pfeffer, S., Cuellar, L.K., Mangold, A.V., Förster, F., 2012. PyTom: a python-based toolbox for localization of macromolecules in cryo-electron tomograms and subtomogram analysis. *J. Struct. Biol.* 178, 177–188.
- Hutchings, J., Stancheva, V., Miller, E.A., Zanetti, G., 2018. Subtomogram averaging of COPII assemblies reveals how coat organization dictates membrane shape. *Nat. Commun.* 9, 4154.
- Koster, A.J., Grimm, R., Typke, D., Hegerl, R., Stoschek, A., Walz, J., Baumeister, W., 1997. Perspectives of molecular and cellular electron tomography. *J. Struct. Biol.* 120, 276–308.
- Kremer, J.R., Mastronarde, D.N., McIntosh, J.R., 1996. Computer visualization of three-dimensional image data using IMOD. *J. Struct. Biol.* 116, 71–76.
- Kühlbrandt, W., 2014. Cryo-EM enters a new era. *Elife* 3, e03678.
- Kürner, J., Frangakis, A.S., Baumeister, W., 2005. Cryo-electron tomography reveals the cytoskeletal structure of *Spiroplasma melliferum*. *Science* 307, 436–438.
- Li, X., Mooney, P., Zheng, S., Booth, C.R., Braunfeld, M.B., Gubbens, S., Agard, D.A., Cheng, Y., 2013. Electron counting and beam-induced motion correction enable near-atomic-resolution single-particle cryo-EM. *Nat. Methods* 10, 584–590.
- Lopez-Garrido, J., Ojčić, N., Khanna, K., Wagner, F.R., Villa, E., Endres, R.G., Pogliano, K., 2018. Chromosome translocation inflates *Bacillus* forespores and impacts cellular morphology. *Cell* 172, 758–770 e714.
- Mahamid, J., Pfeffer, S., Schaffer, M., Villa, E., Danev, R., Cuellar, L.K., Förster, F., Hyman, A.A., Plitzko, J.M., Baumeister, W., 2016. Visualizing the molecular sociology at the HeLa cell nuclear periphery. *Science* 351, 969–972.
- Marko, M., Hsieh, C., Schalek, R., Frank, J., Mannella, C., 2007. Focused-ion-beam thinning of frozen-hydrated biological specimens for cryo-electron microscopy. *Nat. Methods* 4, 215–217.
- Martinez-Sanchez, A., Kochovski, Z., Laugks, U., zum Alten Borgloh, J.M., Chakraborty, S., Pfeffer, S., Baumeister, W., Lucić, V., 2020. Template-free detection and classification of membrane-bound complexes in cryo-electron tomograms. *Nat. Methods* 1–8.
- Mastronarde, D.N., 2005. Automated electron microscope tomography using robust prediction of specimen movements. *J. Struct. Biol.* 152, 36–51.
- McIntosh, R., Nicastro, D., Mastronarde, D., 2005. New views of cells in 3D: an introduction to electron tomography. *Trends Cell Biol.* 15, 43–51.
- McMullan, G., Faruqi, A.R., Henderson, R., 2016. Direct electron detectors. *Methods Enzymol.* 579, 1–17.
- Melia, C.E., Bharat, T.A.M., 2018. Locating macromolecules and determining structures inside bacterial cells using electron cryotomography. *Biochim. Biophys. Acta Protein Proteomics* 1866, 973–981.
- Nicastro, D., Frangakis, A.S., Typke, D., Baumeister, W., 2000. Cryo-electron tomography of neurospora mitochondria. *J. Struct. Biol.* 129, 48–56.
- Noble, A.J., Dandey, V.P., Wei, H., Brasch, J., Chase, J., Acharya, P., Tan, Y.Z., Zhang, Z., Kim, L.Y., Scapin, G., et al., 2018. Routine single particle CryoEM sample and grid characterization by tomography. *Elife* 7.
- Nogales, E., Scheres, S.H., 2015. Cryo-EM: a unique tool for the visualization of macromolecular complexity. *Mol. Cell* 58, 677–689.
- O'Reilly, F.J., Xue, L., Graziadei, A., Sinn, L., Lenz, S., Tegunov, D., Blötz, C., Hagen, W.J., Cramer, P., Stülke, J., et al., 2020. In-cell Architecture of an Actively Transcribing-Translating Expressome. *bioRxiv*.
- Park, D., Lara-Tejero, M., Waxham, M.N., Li, W.W., Hu, B., Galan, J.E., Liu, J., 2018. Visualization of the type III secretion mediated *Salmonella*-host cell interface using cryo-electron tomography. *Elife* 7.
- Patla, I., Volberg, T., Elad, N., Hirschfeld-Warneken, V., Grashoff, C., Fassler, R., Spatz, J.P., Geiger, B., Medalia, O., 2010. Dissecting the molecular architecture of integrin adhesion sites by cryo-electron tomography. *Nat. Cell Biol.* 12, 909–915.
- Pfeffer, S., Woellhaf, M.W., Herrmann, J.M., Förster, F., 2015. Organization of the mitochondrial translation machinery studied in situ by cryoelectron tomography. *Nat. Commun.* 6, 6019.
- Pierson, J., Ziese, U., Sani, M., Peters, P.J., 2011. Exploring vitreous cryo-section-induced compression at the macromolecular level using electron cryotomography: 80S yeast ribosomes appear unaffected. *J. Struct. Biol.* 173, 345–349.
- Russo, C.J., Passmore, L.A., 2014. Ultrastable gold substrates for electron cryomicroscopy. *Science* 346, 1377–1380.
- Salje, J., Zuber, B., Löwe, J., 2009. Electron cryomicroscopy of *E. coli* reveals filament bundles involved in plasmid DNA segregation. *Science* 323, 509–512.
- Schellenberger, P., Kaufmann, R., Siebert, C.A., Hagen, C., Wodrich, H., Grünwald, K., 2014. High-precision correlative fluorescence and electron cryo microscopy using two independent alignment markers. *Ultramicroscopy* 143, 41–51.
- Scheres, S.H., 2012. RELION: implementation of a Bayesian approach to cryo-EM structure determination. *J. Struct. Biol.* 180, 519–530.
- Scheres, S.H., 2014. Beam-induced motion correction for sub-megadalton cryo-EM particles. *Elife* 3, e03665.
- Schorb, M., Gaechter, L., Avinoam, O., Sieckmann, F., Clarke, M., Bebeacua, C., Bykov, Y.S., Sonnen, A.F., Lihl, R., Briggs, J.A., 2017. New hardware and workflows for semi-automated correlative cryo-fluorescence and cryo-electron microscopy/tomography. *J. Struct. Biol.* 197, 83–93.
- Schur, F.K., Obr, M., Hagen, W.J., Wan, W., Jakobi, A.J., Kirkpatrick, J.M., Sachse, C., Kräusslich, H.G., Briggs, J.A., 2016. An atomic model of HIV-1 capsid-SP1 reveals structures regulating assembly and maturation. *Science* 353, 506–508.
- Song, K., Shang, Z., Fu, X., Lou, X., Grigorieff, N., Nicastro, D., 2020. In situ structure determination at nanometer resolution using TYGRESS. *Nat. Methods* 17, 201–208.
- Szweziak, P., Wang, Q., Bharat, T.A., Tsim, M., Löwe, J., 2014. Architecture of the ring formed by the tubulin homologue FtsZ in bacterial cell division. *Elife* 4, e04601.
- Tang, G., Peng, L., Baldwin, P.R., Mann, D.S., Jiang, W., Rees, I., Ludtke, S.J., 2007. EMAN2: an extensible image processing suite for electron microscopy. *J. Struct. Biol.* 157, 38–46.
- Tegunov, D., Cramer, P., 2019. Real-time cryo-electron microscopy data pre-processing with Warp. *Nat. Methods* 16, 1146–1152.
- Turoňová, B., Hagen, W.J., Obr, M., Mosalaganti, S., Beugelink, J.W., Zimmerli, C.E., Kräusslich, H.-G., Beck, M., 2020. Benchmarking tomographic acquisition schemes for high-resolution structural biology. *Nat. Commun.* 11, 1–9.
- Turoňová, B., Schur, F.K., Wan, W., Briggs, J.A., 2017. Efficient 3D-CTF correction for cryo-electron tomography using NovaCTF improves subtomogram averaging resolution to 3.4 angstrom. *J. Struct. Biol.* 199, 187–195.
- von Kügelgen, A., Tang, H., Hardy, G.G., Kureisaite-Ciziene, D., Brun, Y.V., Stansfeld, P.J., Robinson, C.V., Bharat, T.A.M., 2020. In situ structure of an intact lipopolysaccharide-bound bacterial surface layer. *Cell* 180, 348–358 e315.
- Watanabe, R., Buschauer, R., Böhning, J., Audagnotto, M., Lasker, K., Lu, T.W., Boassa, D., Taylor, S., Villa, E., 2019. The in Situ Structure of Parkinson's Disease-Linked LRRK2. *bioRxiv*, p. 837203.
- Weiss, G.L., Kieninger, A.-K., Maldener, I., Forchhammer, K., Pilhofer, M., 2019. Structure and function of a bacterial gap junction analog. *Cell* 178, 374–384 e315.
- Wu, X., Zeng, X., Zhu, Z., Gao, X., Xu, M., 2019. Template-Based and template-free approaches in cellular cryo-electron tomography structural pattern mining. In: *Computational Biology*. Codon Publications.
- Xu, M., Singla, J., Tocheva, E.I., Chang, Y.-W., Stevens, R.C., Jensen, G.J., Alber, F., 2019. De novo structural pattern mining in cellular electron cryotomograms. *Structure* 27, 679–691 e614.
- Zachs, T., Medeiros, J.M., Schertel, A., Weiss, G.L., Hugener, J., Pilhofer, M., 2019. Fully Automated, Sequential Focused Ion Beam Milling for Cryo-Electron Tomography. *bioRxiv*, p. 797514.